



HAL
open science

Path following for a target point attached to a unicycle type vehicle

Yacine Chitour, Salah Laghrouche, Fayez S. Ahmed, Islam Ait-Hammouda

► To cite this version:

Yacine Chitour, Salah Laghrouche, Fayez S. Ahmed, Islam Ait-Hammouda. Path following for a target point attached to a unicycle type vehicle. 2011. hal-00578883v1

HAL Id: hal-00578883

<https://hal.science/hal-00578883v1>

Preprint submitted on 24 Mar 2011 (v1), last revised 4 Jun 2012 (v2)

HAL is a multi-disciplinary open access archive for the deposit and dissemination of scientific research documents, whether they are published or not. The documents may come from teaching and research institutions in France or abroad, or from public or private research centers.

L'archive ouverte pluridisciplinaire **HAL**, est destinée au dépôt et à la diffusion de documents scientifiques de niveau recherche, publiés ou non, émanant des établissements d'enseignement et de recherche français ou étrangers, des laboratoires publics ou privés.

Path following for a target point attached to a unicycle type vehicle

Yacine Chitour^a, Salah Laghrouche^b, Fayez S. Ahmed^b, Islam Ait-Hammouda^c

^aLaboratoire des signaux et systèmes (CNRS - Supélec), 3 rue Joliot-Curie, Plateau de Moulon, 91192 Gif-sur-Yvette Cedex, France
chitour@lss.supelec.fr

^bLaboratoire Systèmes et Transports, Université de Technologie Belfort-Montbéliard, Belfort 90010 France.

^cRenault SAS.

Abstract

In this article, we have addressed the control problem of unicycle path following, using a rigidly attached target point. The initial path following problem has been transformed into a reference trajectory following problem, using saturated control laws and a geometric characterization hypothesis. This hypothesis links the curvature of the path to be followed with the target point. The proposed controller allows global stabilization, without restrictions on initial conditions. The effectiveness of this controller is illustrated through simulations.

1. Introduction

The case of vehicle path following using a "target point" (situated at a distance from the vehicle) is well known in the domain of automatic vehicle guidance. This technique is often used in robotic vehicles with artificial camera vision, where the camera is fixed on the vehicle and the target point (physical or virtual) is situated somewhere in its field of view. This problem has been the subject of many research works in the recent years ([1, 2, 3, 4, 5, 6, 7]). The dominant trend in the contemporary literature is to control either the vehicle's forward velocity (thereby, not controlling the vehicle's orientation), or the instantaneous rotational velocity only. Hence, essentially only one actuator is used.

In [2], a local path following strategy has been proposed, which takes uncertainties into account as well. Their solution is based on a control law that comprises of two terms; an open loop control that allows inversion of the nominal model, and a closed loop control that stabilizes the resultant system. It should be noted that the error dynamics obtained in [2] are expressed in the Frénet frame associated to the followed path (a technique that has also been discussed in ([5])). While the use of Frénet frames of the reference trajectory is convenient, its application is *local*, i.e. the convenience is significant only when the vehicle is close to the path (with respect to a universal constant), as well as positioned and oriented. When such ideal situations are not valid (the vehicle is initially located far from the path),

another controller (e.g. an open loop control) takes over to bring the vehicle in the path's proximity before the primary controller starts operation.

In this paper, we have presented a target point based path following technique for a robot unicycle. The target point has been considered fixed with respect to a point on the vehicle, i.e. the target point is at a fixed distance $d > 0$ from the center of gravity on the axis of the vehicle. Our control objective is to drive the vehicle, such that the target point follows the desired path (see Fig. 1 below). We have assumed that the vehicle's velocity is measured only, and not controlled. This assumption conforms with practical applications, where other intelligent systems control the velocity, (for example, ABS, ESP ([8]).

One of the objectives of this article is to conceive *global* control laws, which are applicable regardless of the initial position and orientation of the vehicle w.r.t. the path to be followed. Hence the problem can be defined as orientation control with a forced forward velocity. Our proposed solution is based on the subsequent consideration: no constraints are imposed on how the reference path is parameterized, therefore, if the path is considered to be the trajectory of a unicycle, the forward velocity of this trajectory can be considered as a supplementary control variable. A similar approach can be found in [1] and [2], where orientation control of a vehicle is under consideration. The authors have achieved this through a dynamic inversion process, implemented using adaptive parametrization of the followed path. In our work, we have chosen the opposite direction, converting the problem of path following into a special case of trajectory following. Furthermore, we have considered the trajectory of the target point as the trajectory of a unicycle. This allows us to express the error dynamics as the difference between the unicycle dynamics defined by the reference path, and the unicycle dynamics defined by the target point. We have thus obtained a controlled system with three dimensional state and two control inputs (the forward velocity of the reference path and the angular velocity of the vehicle) .

Our control law is based upon state feedback with static error control algorithms, along with saturated input technique ([9, 10, 11]). As would be shown further on, the application of bounded inputs is justified by two constraints, (a) to maintain the forward velocity on the reference path uniformly bounded, (b) to focus on controlling the orientation of the unicycle defined by the target point, rather than controlling the orientation of the vehicle. It is worth mentioning that in order to satisfy constraint (b), we have supposed the geodesic curvature of the followed path to be strictly bounded in magnitude by the inverse of the distance d . Application of such type of bounded commands in the same context

(trajectory following of unicycle robots) can be found in [3] . The stability analysis is based on an argument of the Lyapunov type. Our contribution, compared to [3] is the determination of a *strict and global* Lyapunov Function on an appropriate basin of attraction. As a byproduct, we can handle model uncertainties, external perturbations as well as (constant) delays as indicated in a series of remarks preceding the simulation section.

Acknowledgements. The authors thank E. Panteley and W. Pasillas-Lépine for their constructive remarks.

2. Vehicle model and reference trajectory

Let us consider a path γ with geodesic curvature κ_r^* whose absolute value is bounded by $\kappa_{max} \geq 0$. As described in the introduction, we want to parameterize γ as a unicycle trajectory with a forward velocity $u(t)$ such that $\gamma(t) = (p_r(t), q_r(t))$ can be described by the following state equations :

$$\begin{aligned}\dot{p}_r &= u \cos \psi_r, \\ \dot{q}_r &= u \sin \psi_r, \\ \dot{\psi}_r &= u \kappa_r,\end{aligned}\tag{1}$$

where κ_r , is the scalar curvature associated to the parametrization of γ by time t . The relationship between the arclength s of γ and time t for the trajectory (p_r, q_r, ψ_r) is given by $s(t) = s_0 + \int_0^t u(\tau) \tau$. The scalar curvature $\kappa_r(t)$ is hence equal to $\kappa_r^*(s(t))$. For the sake of simplicity, we have assumed in this paper that $u(\cdot)$ is a strictly positive function (i.e., strictly positive forward velocity), and moreover, that the controls u verify $\int_0^\infty u(t) dt = +\infty$. Furthermore, for all $t \geq 0$, we have

$$|\kappa_r(t)| \leq \kappa_{max}.\tag{2}$$

The state equations for the vehicle can be defined as:

$$\begin{aligned}\dot{x} &= V_x \cos \psi, \\ \dot{y} &= V_x \sin \psi, \\ \dot{\psi} &= V_x v,\end{aligned}\tag{3}$$

These equations represent the vehicle's motion with a velocity V_x , along the curve defined by the its geodesic curvature

v . This variable will be considered as the second control in the problem. Notice that V_x is not necessarily constant, but simply a continuous function of time, which verifies the following hypothesis: there exist two positive constants $0 < V_{min} \leq V_{max}$, such that for all $t \geq 0$

$$V_{min} \leq V_x(t) \leq V_{max}. \quad (4)$$

Recall that the strict positivity of the lower bound is a necessary assumption to obtain the results of the paper (see, [6] for an explanation of this classical phenomenon).

For the target point, the equations for the coordinates p and q are defined as:

$$\begin{aligned} p &= x + d \cos \psi, \\ q &= y + d \sin \psi. \end{aligned} \quad (5)$$

We will also suppose throughout the paper that

(H1) $d\kappa_{max} < 1$.

This can be considered as a technical condition, or a design constraint for positioning the target point. However, as explained later, condition (H1) turns out to be (almost) necessary to control the system.

The dynamics of the target point can be obtained by deriving the precedent equations

$$\begin{aligned} \dot{p} &= V_x \cos \psi - d V_x \sin \psi v, \\ \dot{q} &= V_x \sin \psi + d V_x \cos \psi v, \\ \dot{\psi} &= V_x v. \end{aligned} \quad (6)$$

The curve defined by the target point is traveled at the following speed:

$$v_d := \sqrt{\dot{p}^2 + \dot{q}^2} = V_x \sqrt{1 + (vd)^2}.$$

Our objective now is to define the dynamics of the target point as those of a unicycle. Therefore, let us consider θ as the angle between the abscissa axis and the velocity vector $(\dot{p}, \dot{q})^T$. One easily gets that $\theta = \psi + \arctan(v)$ and then,

$$\dot{p} = v_d \cos(\theta), \quad \dot{q} = v_d \sin(\theta),$$

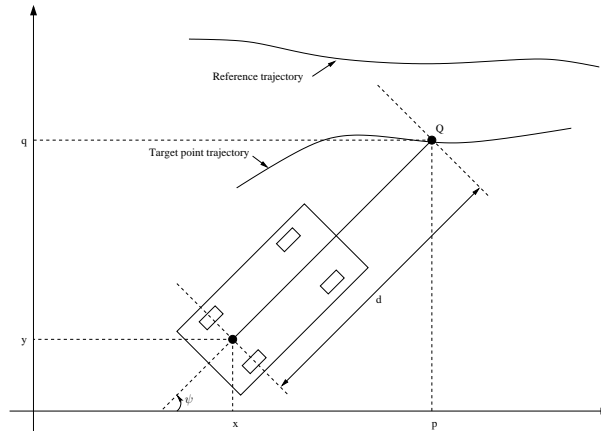


Figure 1: The reference trajectory, the vehicle and its target point.

and the scalar curvature ω is defined by $\omega := \frac{\dot{\theta}}{v_d}$.

Solving these equations, we obtain:

$$\omega = \frac{V_x v}{v_d} + \frac{d \dot{v}}{v_d(1 + (v d)^2)}. \quad (7)$$

Hence the dynamics of the target point (p, q) becomes

$$\begin{aligned} \dot{p} &= v_d \cos \theta, \\ \dot{q} &= v_d \sin \theta, \\ \dot{\theta} &= v_d \omega. \end{aligned} \quad (8)$$

From here on, we will replace v with ω as the new control. Considering equation (7), we obtain the following form:

$$\dot{v} = \frac{1 + (v d)^2}{d} V_x \left[\sqrt{1 + (v d)^2} \omega - v \right], \quad (9)$$

i.e. an ordinary differential equation for the unknown function v . Since the right side of (9) is not globally Lipschitz with respect to v , the solution may only be defined for finite time duration. We will show later on, that a choice of ω under Hypothesis (H1) resolves this problem (see Lemma 1 below).

The error between the target point and the reference curve can be defined as:

$$\begin{aligned} e_p &= p - p_r, \\ e_q &= q - q_r, \\ \xi &= \theta - \psi_r, \end{aligned} \tag{10}$$

and the error dynamics are given by:

$$\begin{aligned} \dot{e}_p &= v_d \cos \theta - u \cos \psi_r, \\ \dot{e}_q &= v_d \sin \theta - u \sin \psi_r, \\ \dot{\xi} &= v_d \omega - \kappa_r u. \end{aligned} \tag{11}$$

The objective, hence, is to determine the control laws, $u(e_p, e_q, \xi)$ and $\omega(e_p, e_q, \xi)$ such that the closed loop system (11) is globally asymptotically stable (GAS for short) with respect to the origin.

Let us first of all perform a variable change on the control, as follows:

$$\begin{aligned} u &= v_d(1 + u_1), \\ \omega &= \kappa_r(1 + u_1) + u_2. \end{aligned} \tag{12}$$

The system that we have to stabilize, becomes:

$$\begin{aligned} \dot{e}_p &= v_d(\cos \theta - \cos \psi_r - u_1 \cos \psi_r), \\ \dot{e}_q &= v_d(\sin \theta - \sin \psi_r - u_1 \sin \psi_r), \\ \dot{\xi} &= v_d u_2. \end{aligned} \tag{13}$$

The following lemma provides bounding conditions on u_1 and u_2 that would guarantee that the differential equation given in (9) is defined for all times $t \geq 0$.

Lemma 1. *Suppose that for all $t \geq 0$, there exists*

$$\frac{|u_1(t)|}{d} + |u_2(t)| \leq \beta_M := \frac{1 - d\kappa_{max}}{d}. \tag{14}$$

Then, the differential equation given by Eq.(9) is defined for all times $t \geq 0$.

Proof of Lemma 1 Let us multiply (9) by v . We obtain:

$$v\dot{v} = \frac{1 + (vd)^2}{d} V_x \left[\sqrt{1 + (vd)^2} v\omega - v^2 \right]. \quad (15)$$

If $v\omega \leq 0$, then $v\dot{v} \leq 0$. If $v\omega > 0$, the precedent equation can be written as:

$$v\dot{v} = \frac{1 + (vd)^2}{d} V_x |v| \left[\frac{\omega^2 + v^2 ((d\omega)^2 - 1)}{\sqrt{1 + (vd)^2} |\omega| + |v|} \right]. \quad (16)$$

In order to guarantee that the right side of (16) is globally Lipschitz with respect to v^2 , it is sufficient to choose u_1, u_2 such that for all $t \geq 0$,

$$(d\omega(t))^2 - 1 \leq 0.$$

Using (12), we can rewrite the equation

$$(d\omega(t))^2 - 1 \leq d^2 (\kappa_{max}(1 + |u_1(t)|) + |u_2(t)|)^2 - 1.$$

For the value of this quantity to be less than zero, it is sufficient that $d(\kappa_{max}(1 + |u_1(t)|) + |u_2(t)|) \leq 1$, and hence for all $t \geq 0$,

$$\frac{|u_1(t)|}{d} + |u_2(t)| \leq \beta_M.$$

In order to verify (14), the controls u_1 et u_2 can be expressed in the following form:

$$\begin{aligned} u_1 &= C_1 \sigma(\cdot), \\ u_2 &= \beta \sigma(\cdot), \end{aligned} \quad (17)$$

with (for instance)

$$(Cond0) \quad 0 < C_1 \leq \frac{d\beta_M}{2}, \quad 0 < \beta \leq \frac{\beta_M}{2}, \quad (18)$$

and σ being equal to the standard saturation function

$$\sigma(x) = \frac{x}{\max(1, |x|)}.$$

■

Since v is bounded, v_d also remains uniformly bounded throughout $t \geq 0$. We can hence change the time by considering $dt' = v_d dt$. To keep the notations simple, we would continue to use t for time. This has no effect on the control laws since our design is based on static feedback (w.r.t. the error).

The error dynamics hence becomes:

$$\begin{aligned} \dot{e}_p &= \cos \theta - \cos \psi_r - u_1 \cos \psi_r, \\ \dot{e}_q &= \sin \theta - \sin \psi_r - u_1 \sin \psi_r, \\ \dot{\xi} &= u_2. \end{aligned} \tag{19}$$

Let us perform the following change of variable corresponding to a time-varying rotation in the frame of the reference trajectory:

$$\begin{aligned} y_1 &= e_p \cos \psi_r + e_q \sin \psi_r, \\ y_2 &= -e_p \sin \psi_r + e_q \cos \psi_r. \end{aligned} \tag{20}$$

The final system can be expressed as

$$\begin{aligned} \dot{y}_1 &= -u_1 + (\cos \xi - 1) + (1 + u_1) \kappa_r y_2, \\ \dot{y}_2 &= \sin \xi - (1 + u_1) \kappa_r y_1, \\ \dot{\xi} &= u_2. \end{aligned} \tag{21}$$

This system of equations greatly resembles the error dynamics obtained for the classic tracking problem of a vehicle using a unicycle, with the forward velocity and the instantaneous rotation velocity of the vehicle body as control variables (cf. [5] et [3]).

We choose the controls u_1 and u_2 as follows:

$$\begin{aligned} u_1 &= C_1 \sigma(My_1), \\ u_2 &= -\beta \sigma\left(\frac{C_0}{\beta} [\xi + \rho \sigma(C_2 y_2)]\right), \end{aligned} \tag{22}$$

with M, C_0, C_2, β as positive constants to be fixed later.

Hence the error dynamics are:

$$\begin{aligned} \dot{y}_1 &= -C_1 \sigma(My_1) + \lambda(t)y_2 + (\cos \xi - 1), \\ \dot{y}_2 &= \sin \xi - \lambda(t)y_1, \\ \dot{\xi} &= -\beta \sigma\left(\frac{C_0}{\beta} [\xi + \rho \sigma(C_2 y_2)]\right), \end{aligned} \tag{23}$$

where $\lambda(t) := (1 + u_1)\kappa_r$. λ is bounded by

$$|\lambda(t)| \leq (3 + C_1)\kappa_{max}. \tag{24}$$

Theorem 1: The system (23) is GAS with respect to 0, with bounds in the norm L_∞ arbitrarily small for the controls u_1 and u_2 , i.e., C_1 and β arbitrarily small.

Proof of Theorem 1

We first have the following result, which is a trivial consequence of the dynamics of $\xi(\cdot)$.

Lemma 2. $\exists t_0 \geq 0 \forall t > t_0 : |\xi(t)| < 2\rho$.

We next impose the following condition.

$$(Cond1) : \quad 3\rho C_0 \leq \beta.$$

This implies that for $t \geq t_0$,

$$\left| \frac{C_0}{\beta} [\xi(t) + \rho \sigma(C_2 y_2(t))] \right| \leq 1.$$

Hence, for $t \geq t_0$, the system (23) becomes:

$$\begin{aligned} y_1 &= -C_1 \sigma(My_1) + \lambda(t)y_2 + (\cos \xi - 1), \\ y_2 &= \sin \xi - \lambda(t)y_1, \\ \dot{\xi} &= -C_0 [\xi + \rho \sigma(C_2 y_2)]. \end{aligned} \quad (25)$$

Let \mathcal{E} be a set of points (y_1, y_2, ξ) such that $|\xi| < 2\rho$. Considering Lemma 2, \mathcal{E} is an open invariant in the system (25). To prove Theorem 1, it is sufficient to form a strict Lyapunov function for (25) on \mathcal{E} . We propose the following candidate function:

$$V(y_1, y_2, \xi) := \frac{y_1^2 + y_2^2}{2} + \frac{F(\xi)y_2}{C_0} + \frac{N}{C_0} \xi^2, \quad (26)$$

with N a positive constant to be determined, and $F(\xi) = \int_0^\xi \frac{\sin s}{s} ds$.

Notice that F is an odd function and if $N > \frac{1}{2C_0}$ then V is positive definite. We next prove that V a strict Lyapunov function for (25) on \mathcal{E} with an appropriate choice of the constants.

Let us suppose from this point on that $\rho \leq \frac{1}{2}$. Therefore, for $\xi \leq 2\rho$:

$$\begin{aligned} 1 - \frac{\xi^2}{6} &\leq \frac{\sin \xi}{\xi} \leq 1 \\ 1 - \frac{\xi^2}{18} &\leq \frac{F(\xi)}{\xi} \leq 1 \end{aligned} \quad (27)$$

From here, it can be deduced that:

$$\begin{aligned} 1 - \frac{2\rho^2}{3} &\leq \frac{\sin \xi}{\xi} \leq 1, \\ 1 - \frac{2\xi^2}{9} &\leq \frac{F(\xi)}{\xi} \leq 1. \end{aligned} \quad (28)$$

The derivative of V along the trajectories of the system is equal to:

$$\begin{aligned} \dot{V} &= - \left[C_1 y_1 \sigma(My_1) + \frac{\lambda(t)F(\xi)}{C_0 \xi} \xi y_1 + \frac{1}{2} \left(N - \frac{F(\xi) \sin \xi}{C_0 \xi^2} \right) \xi^2 \right] \\ &\quad - \left[\frac{1}{2} \left(N - \frac{F(\xi) \sin \xi}{C_0 \xi^2} \right) \xi^2 + \rho N \xi \sigma(C_2 y_2) + \frac{\sin \xi}{\xi} \rho y_2 \sigma(C_2 y_2) \right]. \end{aligned} \quad (29)$$

From equations (24) and (28), it can be seen that the first term of equation (29) is greater or equal to:

$$A(y_1, \xi) := C_1 y_1 \sigma(My_1) - \frac{(3+C_1)\kappa_{max}}{C_0} |\xi y_1| + \frac{1}{2} \left(N - \frac{1}{C_0}\right) \xi^2. \quad (30)$$

Similarly, the second term can be limited by:

$$B(y_2, \xi) := \frac{1}{2} \left(N - \frac{1}{C_0}\right) \xi^2 - \rho N |\xi \sigma(C_2 y_2)| + \left(1 - \frac{2\rho^2}{3}\right) \rho y_2 \sigma(C_2 y_2). \quad (31)$$

Hence, using equations (29), (30) and (31), \dot{V} can be expressed as:

$$\dot{V} \leq -A(y_1, \xi) - B(y_2, \xi). \quad (32)$$

We shall now present two lemmas, and establish the conditions on constants, under which these lemmas would hold true.

Lemma 3. There exist a value of constants, for which the function A is positive definite on $\mathbb{R} \times]-2\rho, 2\rho[$.

Lemma 4. There exist a value of constants, for which the function B is positive definite on $\mathbb{R} \times]-2\rho, 2\rho[$.

Proof of Lemma 3: Let us consider 2 cases:

Case 1: $|y_1| \geq \frac{1}{M}$.

As $|\xi| \leq 2\rho$, we obtain:

$$A \geq |y_1| \left(C_1 - \frac{2\rho\kappa_{max}}{C_0} (3 + C_1) \right). \quad (33)$$

Hence it is sufficient to verify that:

$$C_1 - \frac{2\rho\kappa_{max}}{C_0} (3 + C_1) > 0 \Leftrightarrow C_1 \left(1 - \frac{2\rho\kappa_{max}}{C_0} \right) > \frac{3\kappa_{max}}{C_0} \rho. \quad (34)$$

From here, we obtain a supplementary condition:

$$\frac{\kappa_{max}}{C_0} \rho < 1. \quad (35)$$

This condition, along with *cond1* presented before, is equivalent to:

$$(Cond12) : 9\rho < \frac{\kappa_{max}}{C_0} < \frac{1}{2\rho}.$$

Therefore, C_1 has to be chosen, such that:

$$(Cond3) : C_1 > \frac{\frac{3\kappa_{max}}{C_0} \rho}{\left(1 - \frac{2\rho\kappa_{max}}{C_0}\right)}. \quad (36)$$

Case 2: $|y_1| < \frac{1}{M}$.

As the saturation is no longer activated, A reduces to a quadratic form. To prove that it is positive definite, it is sufficient that

$$\begin{pmatrix} N - \frac{1}{C_0} \\ C_1 M & -\frac{\kappa_{max}(3+C_1)}{2C_0} \\ -\frac{\kappa_{max}(3+C_1)}{2C_0} & N - \frac{1}{C_0} \end{pmatrix} > 0. \quad (37)$$

Equation (37) gives us:

$$C_1 M \frac{N - \frac{1}{C_0}}{2} > \left(-\frac{\kappa_{max}(3+C_1)}{2C_0}\right)^2. \quad (38)$$

Therefore, M should be chosen such that:

$$(Cond4) : M > \frac{\kappa_{max}^2(3+C_1)^2}{2C_0^2 C_1 \left(N - \frac{1}{C_0}\right)}. \quad (39)$$

■

Proof of Lemma 4: B can be expressed in the following manner:

$$B = \left(1 - \frac{2\rho^2}{3}\right) \left(y_2 - \frac{\sigma(C_2 y_2)}{C_2}\right) \sigma(C_2 y_2) + \frac{\rho}{C_2} D(\sigma(C_2 y_2), \xi), \quad (40)$$

where

$$D(z, \xi) := \left(1 - \frac{2\rho^2}{3}\right) z^2 - C_2 N |\xi z| + \frac{C_2}{\rho} \left(N - \frac{1}{C_0}\right) \xi^2. \quad (41)$$

It can be seen from equations (40) and (41), that if D is positive definite, then B is positive definite as well, i.e.:

$$\begin{vmatrix} 1 - \frac{2\rho^2}{3} & \frac{-C_2}{2} \\ \frac{-C_2}{2} & \frac{C_2}{\rho} \left(N - \frac{1}{C_0} \right) \end{vmatrix} > 0. \quad (42)$$

From here, we obtain a new condition on ρ :

$$(Cond5) : \frac{\left(1 - \frac{2\rho^2}{3}\right)}{\rho} > \frac{C_2 N^2}{4 \left(N - \frac{1}{C_0}\right)}. \quad (43)$$

Therefore, to prove the theorem 1, it has to be shown that there exist constants $C_0, C_1, C_2, M, N, \rho$, such that conditions (Cond12) and (cond5) are met. In practice, C_0 and C_2 are given fixed positive values, and then N is fixed such that $N > \frac{1}{C_0}$. Then, ρ is chosen, small enough to satisfy conditions (cond2) and (cond5). Finally, C_1 and M are chosen so that they satisfy respectively conditions (cond3) and (cond4). ■

The results presented above can be improved in the following directions

Remark 1. *Having a strict Lyapunov function allows us to extend the precedent results to cases in which external perturbations exist. More precisely, it can be shown that (25) is ISS (input-to-state) with respect bounded external perturbations and an upper bound for allowed perturbations can be determined explicitly (as a function of the constants of the problem). In particular, it is interesting to suppose that the reference trajectory curvature κ_r , along with the vehicle velocity V_x are susceptible to measurement noise. Hence the system can be stabilized in the proximity of the reference curve, depending explicitly on the magnitude of noise. In the following section, we will present simulation results, both with and without perturbations on κ_r .*

Remark 2. *One limitation of our control laws is that we have used instantaneous measures of κ_r . In the case where the measurement discontinuity is finite, κ_r can be replaced by the following approximation:*

$$\frac{\Psi_r(t) - \Psi_r(t-h)}{h},$$

with h small enough that asymptotic stabilization towards the reference trajectory can be achieved. If one has an a priori bound on the derivative of κ_r , then the above convergence argument carries over for h small enough.

Remark 3. *It is possible not to bound the control u_2 as defined in (22) but to simply use*

$$u_2 = -C_0 [\xi + \rho\sigma(C_2 y_2)].$$

The proof of the non-explosion of (9) is slightly modified.

3. Simulations

In this section, we have presented two simulation cases, based on the following values:

$$d = 2 \text{ m}, \kappa_{max} = 0,02 \text{ m}^{-1}, V_x = 15 \text{ m}\cdot\text{s}^{-1}.$$

We have chosen $d\kappa_{max}$ much smaller than 1 in order to emphasize upon significant initial conditions (in particular, $\xi(0)$ close to π) so that the resultant illustrations highlight our claim. Simulations for the case of $d\kappa_{max}$ close to 1 have been presented in [12], where Remark 3 has been taken into consideration. The initial conditions imposed upon the error are

$$e_p(0) = e_q(0) = 10 \text{ m}, \xi(0) = 9\pi/10.$$

In the first case, the path γ to be followed is defined by the geodesic curvature κ_r (see Fig. 2). Notice that κ_r is not continuous. The reference trajectories, of the vehicle and of the target point are shown together in Figure 3. We can see that the target point trajectory converges on the path in approximately 7 sec. (see Fig. 4). The curves of the control function are given in Fig. 5 and Fig. 6.

In order to illustrate the robustness of our control laws, we have considered a second case where a white noise of amplitude of 5% of κ_{max} is superposed on the geodesic curvature κ_r (see Fig. 7). Again we see that the target point trajectory converges well on path, in approximately 7 sec. (see Figs. 8 and 9). The control curves, u et v , are given in Fig. 10 and Fig. 11.

4. Conclusion

In this article, we have addressed the problem of path following using a target point rigidly attached to a unicycle type vehicle, by controlling only the orientation of the vehicle. The main idea was to consider the parametrization of the followed path as an additional input for the system defined by the error dynamics. Control laws using saturation have been determined in order to achieve global stabilization (i.e., without restrictions on initial conditions) under a (necessary) geometric characterization hypothesis, which relates the followed path with the target point position. This approach can also be extended to the cases where there are external perturbations or uncertainties in the model. Future work directions aim at addressing similar issues with more elaborate car models.

References

- [1] L. Consolini, A. Piazzzi, M. Tosques, Motion planning for steering car-like vehicles, in: European Control Conference, Porto, Portugal, 2001.
- [2] L. Consolini, A. Piazzzi, M. Tosques, A dynamic inversion based controller for path following of car-like vehicles, in: Proc. IFAC world congress, Barcelona, Spain, 2002.
- [3] Z. Jiang, E. Lefeber, H. Nijmeijer, Saturated stabilization and tracking of a nonholonomic mobile robot, *Systems & Control Letters* 42 (2001) 327–332.
- [4] Y. Kanayama, Two dimensional wheeled vehicle kinematics, in: Proc. International conference on robotics and automation, San Diego, California, USA, 1994, pp. 64–77.
- [5] P. Morin, C. Samson, Trajectory tracking for non-holonomic vehicles: overview and case study, in: Proc. Fourth International Workshop on Robot Motion and Control, Puzczykowo, Poland, 2004, pp. 139–153.
- [6] C. Samson, Control of chained systems application to path following and time-varying point-stabilization of mobile robots.
- [7] C. Samson, K. Ait-Abderrahim, Feedback control of a nonholonomic wheeled cart in cartesian space, in: Proc. International conference on robotics and automation, Sacramento, California, USA, 1991.
- [8] W. Pasillas-Lepine, Hybrid modelling and limit cycle analysis for a class of anti-lock brake algorithms, in: International Symposium on Advanced Vehicle Control, Arnhem, The Netherlands, 2004.
- [9] A. Teel, Global stabilization and restricted tracking for multiple integrators with bounded controls, *Systems and Control Letters* 40 (1995) 165–171.
- [10] W. Liu, Y. Chitour, E. Sontag, On finite-gain stabilizability of linear systems subject to input saturation, *SIAM J. Control Optimimization* 34 (04).
- [11] Y. Chitour, W. Liu, E. Sontag, On the continuity and incremental-gain properties of certain saturated linear feedback loops, *International Journal of Robust Nonlinear Control* 5 (5).

- [12] I. Ait-Hammouda, Y. Chitour, S. Laghrouche, Global path following of car models with front point, In preparation.
- [13] C. G. L. Bianco, A. Piazzzi, Optimal trajectory planning with quintic g^2 -splines, in: Proceedings of the IEEE Intelligent Vehicles Symposium, Dearborn, MI, USA, 2000.
- [14] Z. Jiang, H. Nijmeijer, Tracking control of mobile robots: A case study in backstepping, *Automatica* 33 (1997) 1393–1399.
- [15] A. Levant, Sliding order and sliding accuracy in sliding mode control, *International Journal of Control* 58 (06).
- [16] A. Levant, Higher-order sliding modes, differentiation and output-feedback control, *International Journal of Control* 46 (09).

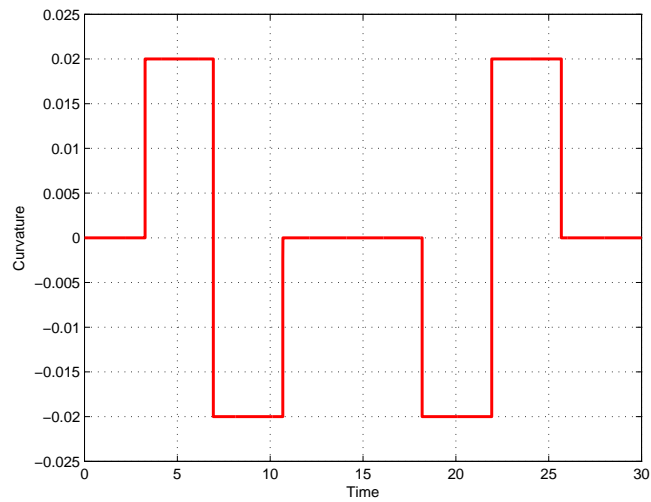


Figure 2: curvature κ_r

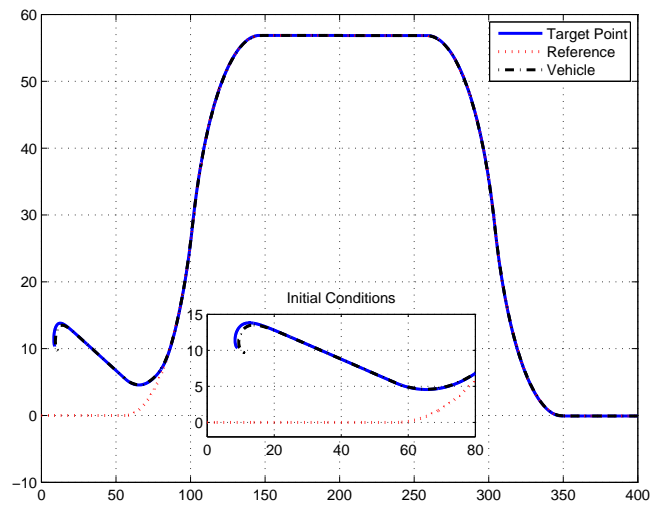


Figure 3: Reference trajectory, of the vehicle and its target point (Case 1: Without perturbations)

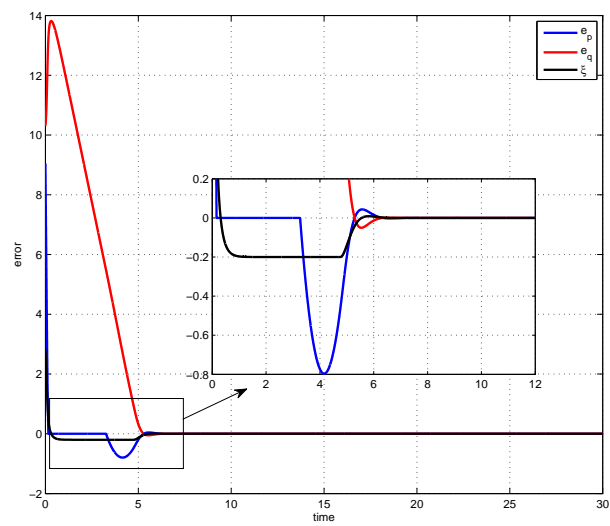


Figure 4: Errors e_p , e_q et ξ

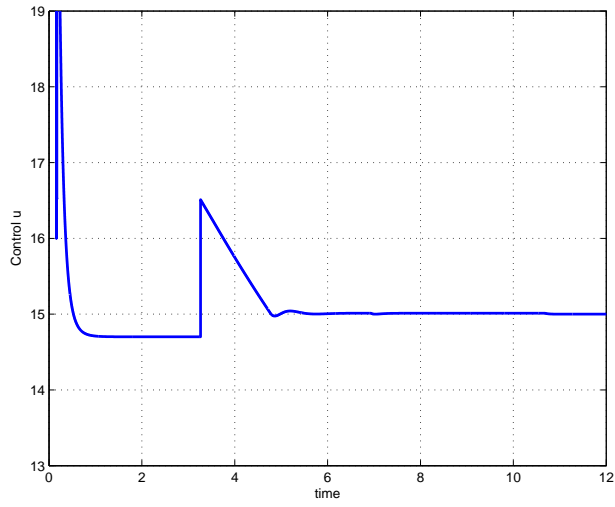


Figure 5: Control u

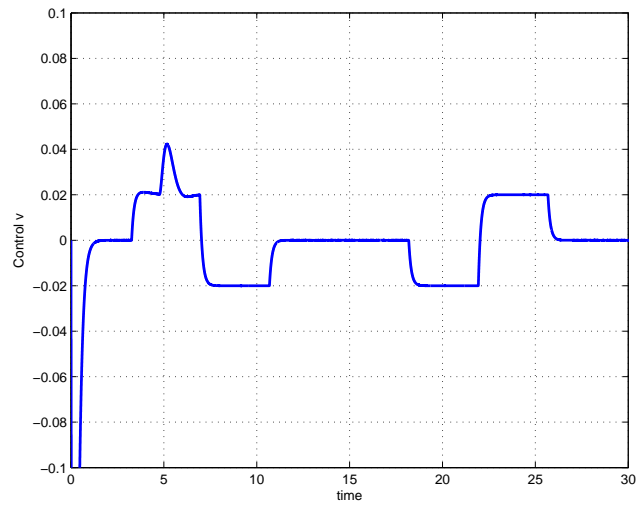


Figure 6: Control v

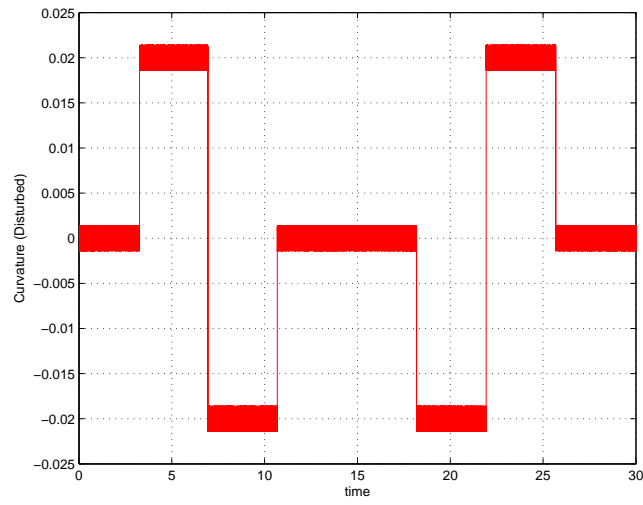


Figure 7: curvature κ_r (Perturbed)

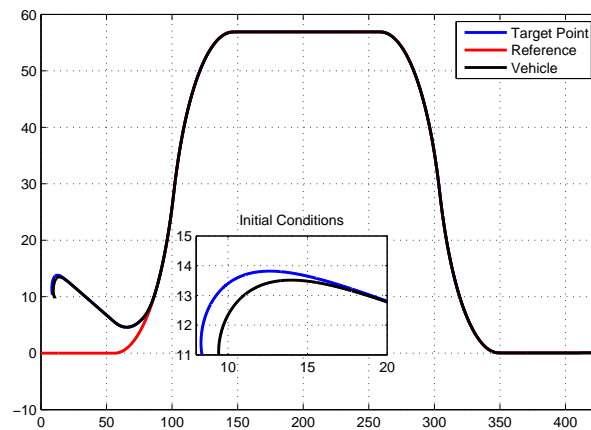


Figure 8: Reference trajectory, of the vehicle and its target point (Case 2: With perturbations)

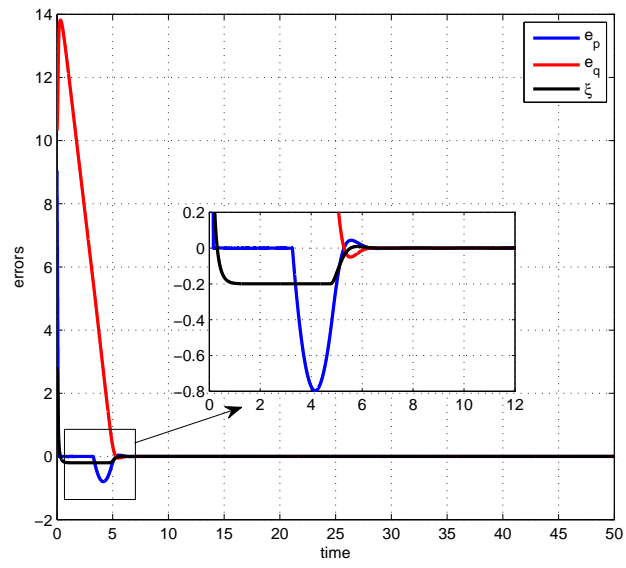


Figure 9: Errors e_p , e_q et ξ (with perturbations)

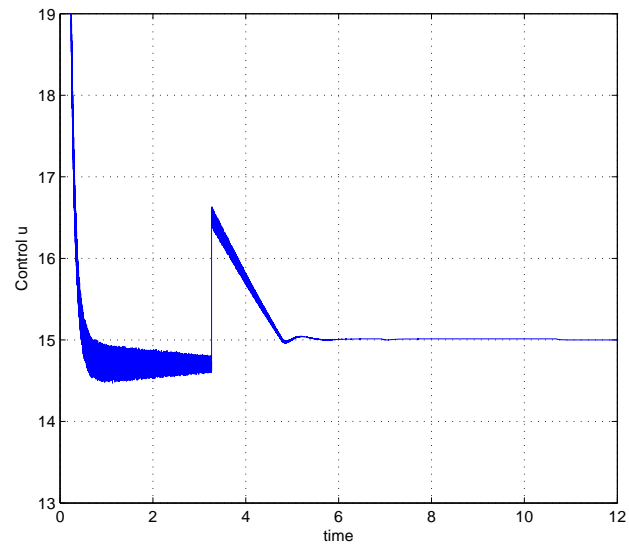


Figure 10: control u (with perturbations)

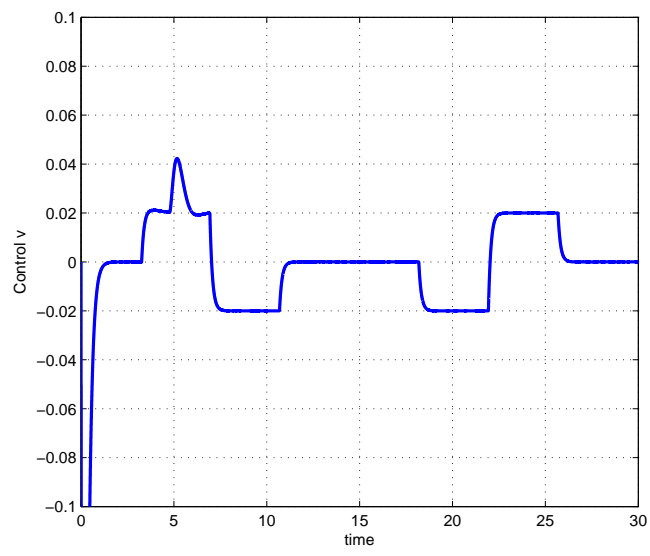


Figure 11: control v (with perturbations)